Influence of Structural Variation on the Anticancer Activity of RAPTA-Type Complexes: ptn versus pta

Anna K. Renfrew,[†] Andrew D. Phillips,[†] Alexander E. Egger,[†,‡] Christian G. Hartinger,[†,‡] Sylvain S. Bosquain,[§] Alexey A. Nazarov,[†] Bernhard K. Keppler,[‡] Luca Gonsalvi,[§] Maurizio Peruzzini,[§] and Paul J. Dyson*[,†]

Institut des Sciences et Ingénierie Chimiques, Ecole Polytechnique Fédérale de Lausanne (EPFL), CH-1015 Lausanne, Switzerland, Institute of Inorganic Chemistry, University of Vienna, Währinger Strasse 42, 1090 Vienna, Austria, and Istituto di Chimica dei Composti Organometallici, Consiglio Nazionale delle Ricerche (ICCOM-CNR), Via Madonna del Piano 10, 50019 Sesto Fiorentino, Firenze, Italy

Received September 16, 2008

A series of compounds of the general formula [M(η^6-arene)(ptn)Cl]X (M = Ru, Os; arene = *p*-cymene, benzene, toluene, hexamethylbenzene; ptn = 3,7-dimethyl-7-phospha-1,3,5-triazabicyclo[3.3.1]nonane; X = Cl^-, BF_4^-) have been prepared and characterized spectroscopically. X-ray diffraction was additionally used to characterize four of the complexes in the solid state. The hydrolysis of the compounds was studied, and their cytotoxicity was evaluated in A2780 ovarian cancer cells and found to be comparable to that of known RAPTA complexes based on 7-phospha-1,3,5-triazatricyclo[3.3.1.1]decane (pta). The reactivity of the complexes toward double-stranded oligonucleotides and the model protein ubiquitin was investigated using Fourier transform ion cyclotron resonance mass spectrometry (FT-ICR-MS) and gel electrophoresis, demonstrating a strong preference for the formation of covalent adducts with the protein. Correlations among compound structure, hydrolysis, biomolecular interactions, and cytotoxicity are established.

Introduction

Cisplatin is currently one of the most widely used chemotherapeutic agents for the treatment of cancer, being applied in over 50% of therapy schemes.[1] However, its activity is impeded by considerable side effects and a high incidence of drug resistance. A large number of cisplatin analogues have been developed with improved properties, although secondary effects continue to present major problems and to date only two compounds, carboplatin and oxaliplatin, have progressed to worldwide clinical use.[2,3]

In recent years, increasing interest has turned to the development of non-platinum inorganic drugs, prominent research being based on ruthenium, gallium, titanium, cobalt, iron, and gold complexes.[4−10] Ruthenium complexes have emerged as an attractive alternative due to their low general toxicity, probable different mode of action, and diverse synthetic chemistry. Moreover, certain ruthenium compounds have been found to display a selectivity toward cancerous cells higher than that of platinum drugs, leading to reduced side effects, and this selectivity may be due to their ability to bind to the iron delivery protein transferrin.[1,11,12] Two ruthenium(III)-based drugs, KP1019[13] and NAMI-A,[14] have currently completed phase I clinical trials. Both complexes behave quite differently from cisplatin in vivo; NAMI-A has been shown to be a strong inhibitor of metastasis while having little effect on primary tumors,[15] and KP1019 effectively reduces colorectal tumors where cisplatin shows essentially no activity.[13]

More recently, investigations into the anticancer activity of organometallic Ru(II) arene compounds have started to gain attention.[16] Different concepts have been followed, including the development of mono- and bifunctional compounds, targeted

* To whom correspondence should be addressed. E-mail: paul.dyson@epfl.ch.
† Ecole Polytechnique Fédérale de Lausanne (EPFL).
‡ University of Vienna.
§ Consiglio Nazionale delle Ricerche (ICCOM-CNR).

(1) Jakupec, M. A.; Galanski, M.; Arion, V. B.; Hartinger, C. G.; Keppler, B. K. *Dalton Trans.* **2008**, 183–194.
(2) Gschwind, A.; Fischer, O. M.; Ullrich, A. *Nat. Rev. Cancer* **2004**, *4*, 361–370.
(3) Kay, P. *Semin. Oncol. Nurs.* **2006**, *22*, 1–4.
(4) Schatzschneider, U.; Metzler-Nolte, N. *Angew. Chem., Int. Ed.* **2006**, *45*, 1504–1507.
(5) Ang, W. H.; Dyson, P. J. *Eur. J. Inorg. Chem.* **2006**, 4003–4018.
(6) Nguyen, A.; Vessieres, A.; Hillard, E. A.; Top, S.; Pigeon, P.; Jaouen, G. *Chimia* **2007**, *61*, 716–724.
(7) Leyva, L.; Sirlin, C.; Rubio, L.; Franco, C.; Le Lagadec, R.; Spencer, J.; Bischoff, P.; Gaiddon, C.; Loeffler, J.-P.; Pfeffer, M. *Eur. J. Inorg. Chem.* **2007**, 3055–3066.
(8) Bruijnincx, P. C. A.; Sadler, P. J. *Curr. Opin. Chem. Biol.* **2008**, *12*, 197–206.
(9) Casini, A.; Hartinger, C. G.; Gabbiani, C.; Mini, E.; Dyson, P. J.; Keppler, B. K.; Messori, L. *J. Inorg. Biochem.* **2008**, *102*, 564–575.
(10) Strohfeldt, K.; Tacke, M. *Chem. Soc. Rev.* **2008**, *37*, 1174–1187.
(11) Clarke, M. J.; Zhu, F.; Frasca, D. R. *Chem. Rev.* **1999**, *99*, 2511–2533.
(12) Pongratz, M.; Schluga, P.; Jakupec, M. A.; Arion, V. B.; Hartinger, C. G.; Allmaier, G.; Keppler, B. K. *J. Anal. At. Spectrom.* **2004**, *19*, 46–51.
(13) Hartinger, C. G.; Zorbas-Seifried, S.; Jakupec, M. A.; Kynast, B.; Zorbas, H.; Keppler, B. K. *J. Inorg. Biochem.* **2006**, *100*, 891–904.
(14) Rademaker-Lakhai, J. M.; van den Bongard, D.; Pluim, D.; Beijnen, J. H.; Schellens, J. H. *Clin. Cancer Res.* **2004**, *10*, 3717–3727.
(15) Alessio, E.; Mestroni, G.; Bergamo, A.; Sava, G. *Curr. Top. Med. Chem.* **2004**, *4*, 1525–1535.
(16) Allardyce, C. S.; Dyson, P. J.; Ellis, D. J.; Heath, S. L. *Chem. Commun.* **2001**, 1396–1397.
(17) Debreczeni, J. É.; Bullock, A. N.; Atilla, G. E.; Williams, D. S.; Bregman, H.; Knapp, S.; Meggers, E. *Angew. Chem.* **2006**, *45*, 1580–1585.
(18) Ang, W. H.; Daldini, E.; Juillerat-Jeanneret, L.; Dyson, P. J. *Inorg. Chem.* **2007**, *46*, 9048–9050.

10.1021/om800899e CCC: $40.75
Publication on Web 01/27/2009

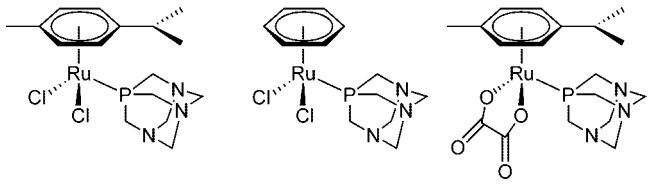

Figure 1. Ru(arene)(pta) complexes RAPTA-C, RAPTA-B, and oxaliRAPTA-C.

approaches and kinase inhibitors,[17−22] and the evaluation of multinuclear ruthenium arene compounds.[23−27]

RAPTA complexes of the general formula [Ru(η^6-arene)(pta)X_2] (X = halide; Figure 1) show relatively low toxicity in vitro, but in vivo studies on RAPTA-C ([Ru(η^6-p-cymene)(pta)Cl_2]) and RAPTA-B ([Ru(η^6-benzene)(pta)Cl_2]) revealed excellent inhibition of metastasis growth in addition to high selectivity and extremely low general toxicity.[28] The pta ligand appears to be essential in endowing the function and selectivity of the RAPTA compound; for example, replacement of pta with the methylated analogue pta-Me^+ greatly increases toxicity in a healthy cell model relative to cancer cells.[28] In contrast, the chloride ligands can be substituted for a bidentate oxalate ligand with very little impact on cytotoxicity, although the rate of reaction with biomolecules is reduced.[29] Replacement of a chloro ligand by a phosphine enables the hydrophobicity and subsequent biological function to be tuned.[30]

In this paper the effect of replacing the pta ligand with a chelating pta analogue, ptn, is described in order to evaluate the effect of forming a P−N chelate complex without significantly altering the water solubility and acid−base properties of the resulting complexes. While examples of Ru(II)−arene complexes containing O or N chelating ligands are known to display cytotoxicity,[31−34] bidentate P,N chelates have not been studied previously, although Pt drugs with hemilabile P,N ligands have been found to display in vitro cytotoxicity equivalent to that of cisplatin.[35]

Scheme 1. Synthesis of [M(η^6-arene)(ptn)Cl]X (M = Ru, Os; X = Cl^-, BF_4^-), Including the NMR Numbering Scheme for the ptn Ligand

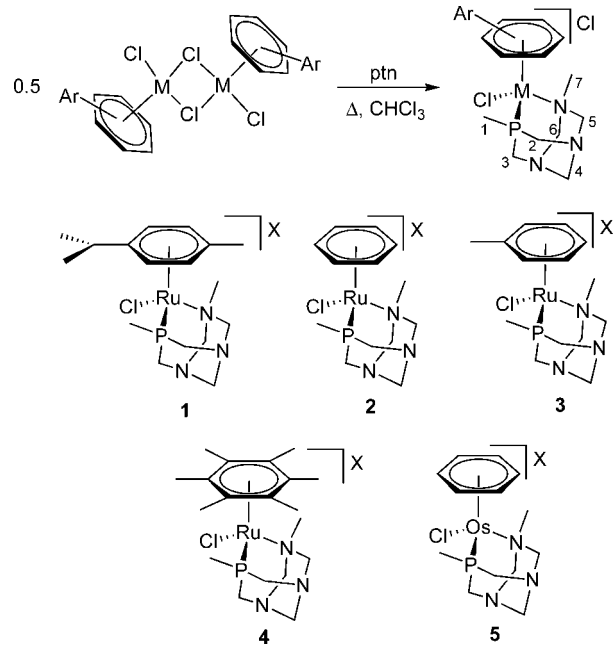

Results and Discussion

A series of ruthenium(II)− and osmium(II)−arene complexes with a ptn ligand were prepared in high yield in a single step (Scheme 1). All complexes are air stable and, with the exception of **4**·Cl, all complexes are highly water soluble (S(**1**, 25 °C) = 0.06 g mL^{-1}) with moderate solubility in chlorinated solvents. The tetrafluoroborate salts, prepared by metathesis of **1**·Cl−**5**·Cl with $NaBF_4$, have higher solubility in chlorinated solvents.

Compounds **1**·Cl−**5**·Cl were characterized by ^{1}H and ^{31}P NMR spectroscopy in D_2O and CD_2Cl_2. ^{1}H−^{1}H COSY and ^{1}H−^{13}C HETCOR spectra of **1**·Cl were used to assign the signals corresponding to the ptn ligand (Scheme 1). ^{1}H−^{15}N correlation and COSY spectra were also recorded for **1**·Cl and **5**·Cl to corroborate peak assignments (see Experimental Section). The ^{31}P NMR spectra of **1**−**5** exhibit a singlet in D_2O and CD_2Cl_2 (Table 1). In the ^{1}H NMR spectrum of **1**, the signals of the *p*-cymene ring are split, indicative of a chiral Ru(II) center. A closed-ring structure is implied by splitting of the methylene groups (Scheme 1), also observed for **2**−**5**. ^{15}N NMR spectra were recorded for complexes **1**·Cl and **5**·Cl; however, no signal corresponding to the chelating nitrogen was observed, possibly because the ligand undergoes a rapid, dynamic opening−closing process involving $\kappa^2 \leftrightarrow \kappa^1$ coordination.

(19) Schmid, W. F.; John, R. O.; Muhlgassner, G.; Heffeter, P.; Jakupec, M. A.; Galanski, M.; Berger, W.; Arion, V. B.; Keppler, B. K. *J. Med. Chem.* **2007**, *50*, 6343–6355.

(20) Schmid, W. F.; John, R. O.; Arion, V. B.; Jakupec, M. A.; Keppler, B. K. *Organometallics* **2007**, *26*, 6643–6652.

(21) Vock, C. A.; Ang, W. H.; Scolaro, C.; Phillips, A. D.; Lagopoulos, L.; Juillerat-Jeanneret, L.; Sava, G.; Scopelliti, R.; Dyson, P. J. *J. Med. Chem.* **2007**, *50*, 2166–2175.

(22) Ang, W. H.; De Luca, A.; Chapuis-Bernasconi, C.; Juillerat-Jeanneret, L.; Lo Bello, M.; Dyson, P. J. *ChemMedChem* **2007**, *2*, 1799–1806.

(23) Mendoza-Ferri, M. G.; Hartinger, C. G.; Eichinger, R. E.; Stolyarova, N.; Severin, K.; Jakupec, M. A.; Nazarov, A. A.; Keppler, B. K. *Organometallics* **2008**, *27*, 2405–2407.

(24) Mendoza-Ferri, M. G.; Hartinger, C. G.; Nazarov, A. A.; Kandioller, W.; Severin, K.; Keppler, B. K. *Appl. Organomet. Chem.* **2008**, *22*, 326–332.

(25) Schmitt, F.; Govindaswamy, P.; Suess-Fink, G.; Ang, W. H.; Dyson, P. J.; Juillerat-Jeanneret, L.; Therrien, B. *J. Med. Chem.* **2008**, *51*, 1811–1816.

(26) Auzias, M.; Therrien, B.; Suess-Fink, G.; Stepnicka, P.; Ang, W. H.; Dyson, P. J. *Inorg. Chem.* **2008**, *47*, 578–583.

(27) Therrien, B.; Suess-Fink, G.; Govindaswamy, P.; Renfrew, A. K.; Dyson, P. J. *Angew. Chem., Int. Ed.* **2008**, *47*, 3773–3776.

(28) Scolaro, C.; Bergamo, A.; Brescacin, L.; Delfino, R.; Cocchietto, M.; Laurenczy, G.; Geldbach, T. J.; Sava, G.; Dyson, P. J. *J. Med. Chem.* **2005**, *48*, 4161–4171.

(29) Casini, A.; Mastrobuoni, G.; Ang, W. H.; Gabbiani, C.; Pieraccini, G.; Moneti, G.; Dyson, P. J.; Messori, L. *ChemMedChem* **2007**, *2*, 631–635.

(30) Scolaro, C.; Chaplin, A. B.; Hartinger, C. G.; Bergamo, A.; Cocchietto, M.; Keppler, B. K.; Sava, G.; Dyson, P. J. *Dalton Trans.* **2007**, 5065–5072.

(31) Habtemariam, A.; Melchart, M.; Fernandez, R.; Parsons, S.; Oswald, I. D. H.; Parkin, A.; Fabbiani, F. P. A.; Davidson, J. E.; Dawson, A.; Aird, R. E.; Jodrell, D. I.; Sadler, P. J. *J. Med. Chem.* **2006**, *49*, 6858–6868.

(32) John, R. O.; Arion, V. B.; Jakupec, M. A.; Keppler, B. K. Ruthenium(II)-arene complex with heterocyclic ligands as prospective antitumor agent. In *Metal Ions in Biology and Medicine*; Alpoim, M. C., Morais, P. V., Santos, M. A., Cristóvão, A. J., Centeno, J. A., Collery, P., Eds.; Editions John Libbey Eurotext: Montrouge, 2006; Vol. 9, pp 40−45.

(33) Peacock, A. F. A.; Parsons, S.; Sadler, P. J. *J. Am. Chem. Soc.* **2007**, *129*, 3348–3357.

(34) Vock, C. A.; Renfrew, A. K.; Scopelliti, R.; Juillerat-Jeanneret, L.; Dyson, P. J. *Eur. J. Inorg. Chem.* **2008**, 1661–1671.

(35) Habtemariam, A.; Sadler, P. J. *Chem. Commun.* **1996**, 1785–1786.

Table 1. ^{31}P NMR Spectroscopic Data for 1·Cl−5·Cl

	D_2O solvent	CD_2Cl_2 solvent
1·Cl	−27.8	−33.1[a]
2·Cl	−28.7	−31.7
3·Cl	−28.0	−31.4
4·Cl	−31.7	−32.4
5·Cl	−77.8	−80.0[b]
ptn	−89.0	−91.2

[a] For **1**·BF_4. [b] Solvent $CDCl_3$.

Structural Characterization of 1·BF_4−4·BF_4 in the Solid State. Crystals of **1**·BF_4−**4**·BF_4 suitable for X-ray diffraction were obtained via slow diffusion (see the Experimental Section for details). Complex **2**·BF_4 crystallized with two symmetry-independent molecules within the unit cell. Essentially, both entities have identical metric parameters; the main difference lies in the rotation of the arene along the Ru−centroid axis, one molecule featuring an eclipsing of an arene carbon with the Ru−Cl bond.

Complexes **1**·BF_4−**4**·BF_4 represent a unique series of complexes, in which the chelating κ^2P,N ligand forms a six-membered ring with Ru containing no unsaturated bonds. A survey of the CSD shows that all Ru compounds with the P,N six-membered ring feature either a substituted pyridine or the incorporation of a phenyl group or imino functionality into the backbone of the ligand to enforce rigidity.[36] In contrast, the rigidity of the ptn molecule stems from the incorporation of a tightly constrained CH_2 bridgehead in the central core of the ligand, indicated by the small N−C(H_2)−N angle of ca. 112°. The CSD also shows that the number of η^6-arene-bound Ru complexes featuring a six-membered κ^2P,N chelating ligand is significantly lower than the corresponding five-membered-ring-containing complexes: 53 versus 13. The four complexes shown in Figure 2 exhibit the typical three-legged piano-stool geometry associated with Ru(II)−arene complexes. Not including the substituents on the arene, the local C_s symmetry is observable from bisection of the Ru−Cl bond, which divides through the middle of the ptn ligand where the mirror plane contains the N−CH_2−N bridgehead fragment. The positioning of the ptn with respect to the arene−Ru−Cl unit is similar in all complexes, where a slight turning about the P−N(terminal) axis is observed, and the bulkiest arene, η^6-C_6Me_6, induces the largest degree of rotation. Metric parameters pertaining to the P center and terminal nitrogen are unreliable due to a positional disordering of the κ^2-ptn ligand where the P and terminal N centers overlap with occupancies ranging from 0.50:0.50 in **4**·BF_4 to 0.89:011 in **1**·BF_4. Analysis of the electron density difference maps reveals that the disorder is restricted to a single plane comprising P, N, and Ru atoms, and no disorder is present in the orthogonal direction. The bridgehead carbon center, N−*C*H_2−N, shows no indication of disorder and is rigidly constrained; thus, the Ru···C(H_2) distance is a useful measure of the κ^2-ptn−Ru interaction. The bridge supporting nitrogens also show some degree of bond strain, as indicated by a relatively planar geometry (sum of C−N−C bond angles: average of **1**·BF_4−**4**·BF_4 336.3° versus 331.94° in $N(CH_3)_3$[37] and 330.23° in uncoordinated pta).[38] The P−Ru−N bond angles in complexes **1**·BF_4−**4**·BF_4 range from 79.61(5) to 82.88(9)°. These values represent the lower limit of data relative to other complexes with six-membered rings containing an arene-bound Ru moiety chelated by a κ^2-P,N ligand: 79.35−93.03°. The basic geometry of the complexes is governed by the steric profile of the coordinating arene. For example, **2**·BF_4 with the smallest arene, η^6-C_6H_6, has the shortest Ru−Cl bond lengths (2.398(2) and 2.400(2) Å), Ru−arene(centroid) length (2.200(8) Å), and Ru−ptn(bridgehead CH_2) distance (4.325(6) Å). The complex containing the most sterically demanding arene, η^6-C_6Me_6, has the longest Ru−P (4.400(5) Å) and Ru−Cl distances (2.431(1) Å). The Ru−arene(centroid) distance in **4**·BF_4 is long (1.770(2) Å), despite the hexamethylbenzene ring being the strongest π-donor of the series. The positioning of the ptn ligand with respect to the Cl center shows minor variation (see Table 2), whereas the bond angle associated with the arene can vary up to 5°, which is again related to the steric profile of the coordinating arene. In comparison to the bis-coordinated, nonchelated (η^6-$C_6H_5CH_2CH_2NH_2$-κ^1N)Ru-Cl(pta-κ^1P) complex,[39] which features both P and N centers bound to Ru, the arene distance of 1.701(3) Å is considerably shorter than in **1**·BF_4−**4**·BF_4; however, the Ru−Cl distance in the tethered complex (2.417(2) Å) is comparable.

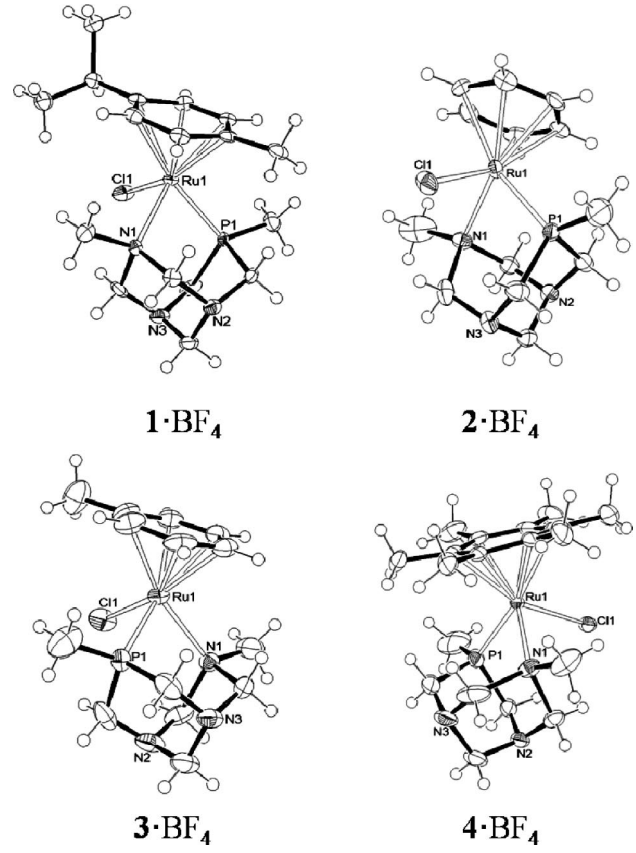

Figure 2. X-ray structures of the cations in **1**·BF_4−**4**·BF_4 with 50% probability thermal ellipsoids (the BF_4^- counterions are omitted for clarity). For **3**·BF_4 only one cation is shown.

Characterization of 1·Cl−5·Cl in Aqueous Solution. The hydrolysis behavior of **1**·Cl−**5**·Cl was studied under pseudopharmacological conditions. Hydrolytic decomposition is central to the mode of action associated with cisplatin[40] and is also thought to be relevant for mono- and dichloro ruthenium(II)−arene based drugs,[41] which undergo rapid hydrolysis in water contain-

(36) Allen, F. H. *Acta Crystallogr., Sect. B: Struct. Sci.* **2002**, *B58*, 380–388.

(37) Boese, R.; Blaser, D.; Antipin, M. Y.; Chaplinski, V.; de Meijere, A. *Chem. Commun.* **1998**, 781–782.

(38) Marsh, R. E.; Kapon, M.; Hu, S.; Herbstein, F. H. *Acta Crystallogr., Sect. B: Struct. Sci.* **2002**, *B58*, 62–77.

(39) Scolaro, C.; Geldbach, T. J.; Rochat, S.; Dorcier, A.; Gossens, C.; Bergamo, A.; Cocchietto, M.; Tavernelli, I.; Sava, G.; Rothlisberger, U.; Dyson, P. J. *Organometallics* **2006**, *25*, 756–765.

(40) Lippert, B., *Cisplatin: Chemistry and Biochemistry of a Leading Anticancer Drug*, 1st ed.; Helvetica Chimica Acta/Wiley-VCH: Zürich/Weinheim, 1999; p 576.

(41) Scolaro, C.; Hartinger, C. G.; Allardyce, C. S.; Keppler, B. K.; Dyson, P. J. *J. Inorg. Biochem.* **2008**, *102*, 1743–1748.

Table 2. Selected Bond Lengths (Å) and Angles (deg) for 1·BF$_4$−4·BF$_4$

	1·BF$_4$	2·BF$_4$[b]	3·BF$_4$	4·BF$_4$
Ru−Cl	2.422(2)	2.400(2)	2.423(2)	2.431(1)
		2.398(2)		
Ru−arene(centroid)	1.733(2)	1.724(3)	1.741(3)	1.786(2)
		1.722(3)		
Ru−C[a]	4.377(4)	4.345(9)	4.346(6)	4.398(4)
		4.325(6)		
Ru−N[c]	2.34(2)	2.25(2)	2.28(3)	2.24(3)
	2.26(4)	2.35(4)	2.35(3)	2.31(3)
		2.20(5)		
		2.36(6)		
Ru−P[c]	2.27(1)	2.25(1)	2.27(1)	2.27(1)
	2.25(1)	2.27(1)	2.20(1)	2.25(1)
		2.24(3)		
		2.20(1)		
Cl−Ru−arene(centroid)	121.81(5)	124.0(1)	123.3(1)	120.41(6)
		124.6(1)		
C[a]−Ru−Cl	90.0(1)	92.7(1)	91.8(1)	90.79(4)
		92.2(1)		
C[a]−Ru−arene(centroid)	148.15(6)	143.3(1)	144.9(1)	148.4(1)
		143.2(2)		
Cl−Ru−P[c]	89.0(2)	88.7(1)	87.9(3)	90.4(2)
	88.5(2)	87.1(3)	89.2(3)	90.1(3)
		90.5(2)		
		89.7(6)		
Cl−Ru−N[c]	86.3(6)	88.8(12)	92.7(7)	88.6(7)
	93.9(9)	86.5(12)	89.8(7)	89.5(10)
		88.5(7)		
		93.2(7)		
P−Ru−N[c]	80.6(7)	79.5(14)	81.0(9)	78.2(9)
	77.1(10)	79.9(15)	79.8(8)	77.8(8)
		78.6(6)		
		80.6(9)		
N−C[a]−N	112.0(3)	112.2(5)	112.4(5)	112.8(3)
		110.8(7)		

[a] Denotes the bridgehead carbon position. [b] Two crystallographically independent molecules are present in the unit cell. [c] The value should be treated with caution, due to the disorder of the P1 and N1 positions in the coordinated ptn ligand.

ing 5 mM NaCl (the approximate salt concentration inside a cell).[42] The process is reversed by addition of 100 mM NaCl (corresponding to the salt concentration of blood plasma). However, the ptn-containing complexes are much less prone to hydrolysis. ESI-MS of compounds **1**·Cl−**3**·Cl and **5**·Cl in water provide a strong peak corresponding to the parent cation, [M(η^6-arene)(ptn)Cl]$^+$, the most abundant peak in each spectrum, with the aqua (or potentially hydroxo) complex, [M(η^6-arene)(ptn)(H$_2$O) − H]$^+$, present at ca. 15% relative intensity for **2**·Cl and **3**·Cl and <5% for **1**·Cl and **5**·Cl.

The stability of **1**·Cl−**5**·Cl in D$_2$O (5 mM NaCl) was monitored by ^{1}H and ^{31}P NMR spectroscopy over a prolonged period (in the case of **4**·Cl the solution contained 1% v/v DMSO to aid solubility). Both **1**·Cl and **2**·Cl were found to be remarkably stable in solution, with no evidence of decomposition after 7 days. In the case of **3**·Cl and **5**·Cl, a new species, probably corresponding to the hydrolysis product [M(arene)(ptn)(H$_2$O)]$^{2+}$, is evident in the ^{31}P NMR spectra after 24 h. In addition, a small amount of free arene (<5% intensity) is observed after 3 days, evidenced by ^{1}H NMR spectroscopy. Only **4**·Cl shows significant decomposition with complete disappearance of the original compound after 3 days, accompanied by the formation of two decomposition products in which the arene ligand has been lost, possibly due to the greater steric demand of the η^6-hexamethylbenzene ligand relative to the other arenes.

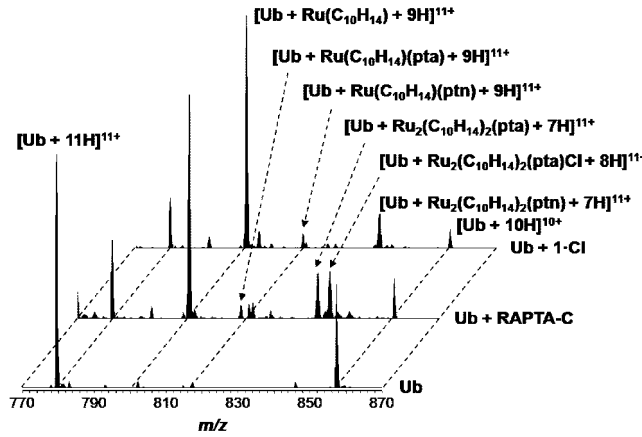

Figure 3. FT-ICR WSIM mass spectra of the reaction mixtures of RAPTA-C and **1**·**Cl** with ubiquitin in a complex to protein ratio of 2:1 after 72 h incubation.

Reactivity of 1·Cl −5·Cl toward Model Biomolecular Targets. Proteins are known to react quickly with metallodrugs after intravenous administration, and both human serum albumin and transferrin are considered as important carriers of anticancer metal complexes.[43] In recent years, metal binding to a number of small proteins with a comparatively low number of potential binding sites have been studied by mass spectrometry.[29,44−46] In particular, the model protein ubiquitin was found useful for this approach, and metal binding sites can even be determined by tandem mass spectrometry.[46] The reaction of RAPTA-C, **1**·Cl, and **5**·Cl toward ubiquitin was monitored by mass spectrometry. RAPTA-C and **1**·Cl give essentially the same type of conjugates after 72 h incubation (Figure 3). However, initially the reaction of the ptn complex appears to proceed more quickly, with the Ub−Ru(*p*-cymene) adduct being the most abundant peak in the mass spectrum after 24 h. In contrast, for the Os complex **5**·Cl no assignable adducts were observed even after incubation for 72 h.

Most metal-based drugs are thought to act by binding to DNA, thereby preventing replication of the cell.[47] The electron-rich N7 site of guanosine has been identified as the preferred binding site for most inorganic drugs,[48−50] and RAPTA compounds have previously been found to react with guanosine at the N7 site to form [Ru(η^6-arene)(guanosine)(pta)Cl]$^+$ complexes, while displaying very little reactivity toward other bases.[51] In order to determine whether a similar selectivity is exhibited by the ptn complexes, D$_2$O solutions of **1**·Cl, **3**·Cl, and **5**·Cl were incubated at 37 °C with 1 mol equiv of guanosine 5′-monophosphate (GMP) and monitored by ^{1}H and ^{31}P NMR spectroscopy. 1:1 solutions of RAPTA-C in D$_2$O and in 100 mM NaCl in D$_2$O were also studied for comparison.

RAPTA-C reacts rapidly with GMP, with a new species forming after 10 min, evidenced by the change in frequency of

(42) Hartinger, C. G.; Schluga, P.; Galanski, M.; Baumgartner, C.; Timerbaev, A. R.; Keppler, B. K. *Electrophoresis* **2003**, *24*, 2038–2044.
(43) Timerbaev, A. R.; Hartinger, C. G.; Aleksenko, S. S.; Keppler, B. K. *Chem. Rev.* **2006**, *106*, 2224–2248.
(44) Gibson, D.; Costello, C. E. *Eur. Mass Spectrom.* **1999**, *5*, 501–510.
(45) Hartinger, C. G.; Ang, W. H.; Casini, A.; Messori, L.; Keppler, B. K.; Dyson, P. J. *J. Anal. At. Spectrom.* **2007**, *22*, 960–967.
(46) Hartinger, C. G.; Tsybin, Y. O.; Fuchser, J.; Dyson, P. J. *Inorg. Chem.* **2008**, *47*, 17–19.
(47) Reedijk, J. *Chem. Rev.* **1999**, *99*, 2499–2510.
(48) Marcelis, A. T. M.; Reedijk, J. *Recl.: J. R. Neth. Chem. Soc.* **1983**, *102*, 121–129.
(49) Fish, R. H. *Coord. Chem. Rev.* **1999**, *185−186*, 569–584.
(50) Egger, A.; Arion, V. B.; Reisner, E.; Cebrian-Losantos, B.; Shova, S.; Trettenhahn, G.; Keppler, B. K. *Inorg. Chem.* **2005**, *44*, 122–132.

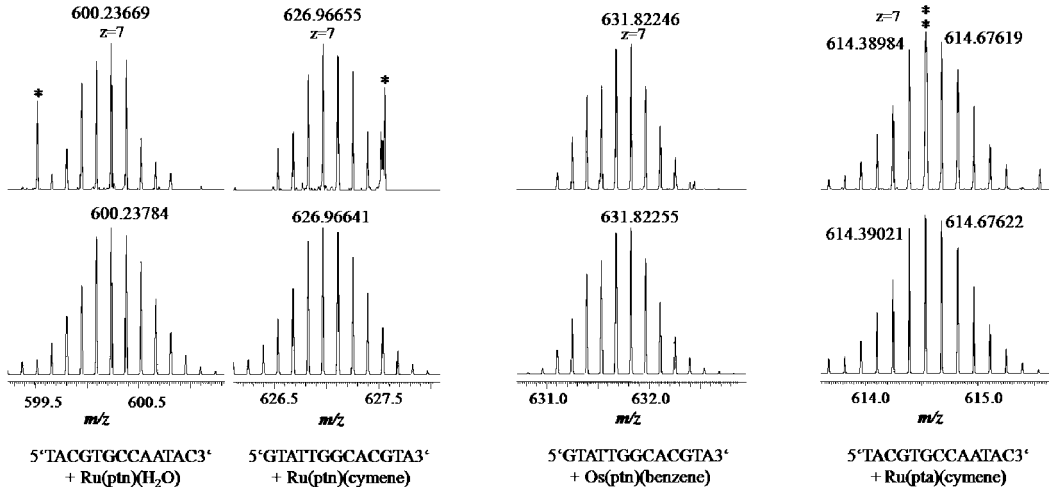

Figure 4. FT-ICR-MS peak patterns (top, experimental; bottom, calculated) of the most abundant 7-fold negatively charged adducts (bottom) resulting from incubation of (from left to right) **1**·Cl, **5**·Cl,and RAPTA-C with ds(5′GTATTGGCACGTA) in a complex to oligonucleotide ratio of 5:1. The double-stranded oligonucleotide was separated into its complementary single strands (GTATTGGCACGTA and TACGTGCCAATAC) during MS. Single asterisks indicate a peak also present in the original oligonucleotide sample. Double asterisks indicate a poorly shaped peak, probably due to overlap with an impurity, and hence the experimental and calculated *m*/*z* values are given for the neighboring peaks.

the H8 proton in the ^{1}H NMR spectrum and of the P atom of the pta ligand in the ^{31}P NMR spectrum. The reaction reaches completion after 4 h, and no new species are formed over 72 h. In the presence of 100 mM NaCl, hydrolysis is suppressed and no reaction with GMP is observed after 3 days.

Compound **1**·Cl does not react with GMP; following 72 h of incubation only unreacted **1**·Cl and GMP are visible in the NMR spectra, with no evidence of hydrolysis or decomposition. In the case of **3**·Cl and **5**·Cl, a new ^{31}P NMR signal attributed to the aqua hydrolysis product is visible after 4 h of incubation; however, there is no evidence for reaction with GMP and the spectra remain unchanged after 24 h. The experiment was repeated with adenosine 5′-monophosphate, but no reaction was observed for **1**·Cl, **3**·Cl, or **5**·Cl over 24 h.

Related [Ru(η^6-arene)(en)Cl]$^+$ compounds have been shown to bind to DNA oligonucleotides, forming monofunctional adducts, selectively binding to guanine following loss of the chloride ligand.[52] Oligomer binding studies using the single-stranded oligomer 5′-ATACATGGTACATA-3′ have been carried out on a series of RAPTA complexes and their osmium analogues, the adducts being analyzed by ESI-MS.[53] The ruthenium compounds were found to form adducts based on either a Ru−arene−pta fragment following the substitution of the chloride ligands or a Ru−pta unit following additional loss of the arene, with a higher percentage of Ru−pta adducts observed for arenes with electron-withdrawing substituents.[39,53] In contrast, the osmium analogues displayed lower reactivity toward DNA, with only Os−arene−pta adducts formed due to the stronger Os−arene bond. Loss of the pta ligand has not been observed, although pta loss on protein binding readily occurs.[29,30]

To determine the reactivity of the ptn complexes relative to those containing pta, with respect to the formation of covalent interactions, the reactions of **1**·Cl, **5**·Cl, and RAPTA-C with the double-stranded oligomer 5′-GTATTGGCACGTA-3′ were assessed by FT-ICR-MS and gel electrophoresis. For each complex, samples were incubated at 1:1 and 5:1 complex to oligomer ratios and analyzed by nESI-FT-ICR-MS after 24 and 72 h. As was observed with the single-stranded oligomer, RAPTA-C reacts to form mainly Ru−arene−pta (up to 70% relative intensity, Figure 4) and smaller amounts of Ru−pta adducts (up to 10%, referenced to unreacted single-stranded 5′-GTATTGGCACGTA-3′, the most abundant peak at charge state 7) with no difference in the spectra after 24 or 72 h at a ratio of 1:1. In comparison **1**·Cl is less reactive, with no adducts formed at a complex to oligonucleotide ratio of 1:1; the intensity of unreacted oligonucleotide remains unchanged, although on increasing the concentration of complex to a 5-fold excess, adducts of ca. 10% relative intensity corresponding to a mono-substituted Ru−arene−ptn fragment are formed after 24 h (Figure 4). Interestingly, this species is no longer present in spectrum recorded after 72 h; instead, species in which the arene has been lost are observed.

Complex **5**·Cl shows very low reactivity toward the oligomer; following 24 h incubation with a 5-fold excess of complex, only a small proportion of the complex had reacted to give an Os−arene−ptn adduct (15% relative intensity, Figure 4). After 72 h of incubation the main peaks in the spectrum remained unchanged. It is worth noting that no signals which could correspond to arene loss were observed, which is in keeping with the stronger Os−arene bond. For the Ru complexes the signal to noise ratio continuously deteriorated, suggesting that the oligonucleotide steadily degraded with time, an effect that could also be due to noncovalent interactions between the complexes and oligonucleotide. Polyacrylamide gel electrophoresis was used to directly determine whether **1**·Cl, **5**·Cl, and RAPTA-C could degrade the oligonucleotide. In agreement with the MS data, gel electrophoresis confirmed that RAPTA-C degraded the oligonucleotide to the greatest extent (Figure 5, top). In contrast, for **1**·Cl a 5-fold excess of the complex is required for a significant degradation of the oligonucleotide (Figure 5, middle) and **5**·**Cl** is the least reactive (Figure 5, bottom).

In Vitro Activity. The in vitro activity of **1**·Cl−**5**·Cl was determined using the MTT test in the ovarian cancer cell line A2780, and antiproliferative activity was found to follow the

(51) Dorcier, A.; Hartinger, C. G.; Scopelliti, R.; Fish, R. H.; Keppler, B. K.; Dyson, P. J. *J. Inorg. Biochem.* **2008**, *102*, 1066–1076.
(52) Morris, R. E.; Aird, R. E.; Murdoch, P. d. S.; Chen, H.; Cummings, J.; Hughes, N. D.; Parsons, S.; Parkin, A.; Boyd, G.; Jodrell, D. I.; Sadler, P. J. *J. Med. Chem.* **2001**, *44*, 3616–3621.
(53) Dorcier, A.; Dyson, P. J.; Gossens, C.; Rothlisberger, U.; Scopelliti, R.; Tavernelli, I. *Organometallics* **2005**, *24*, 2114–2123.

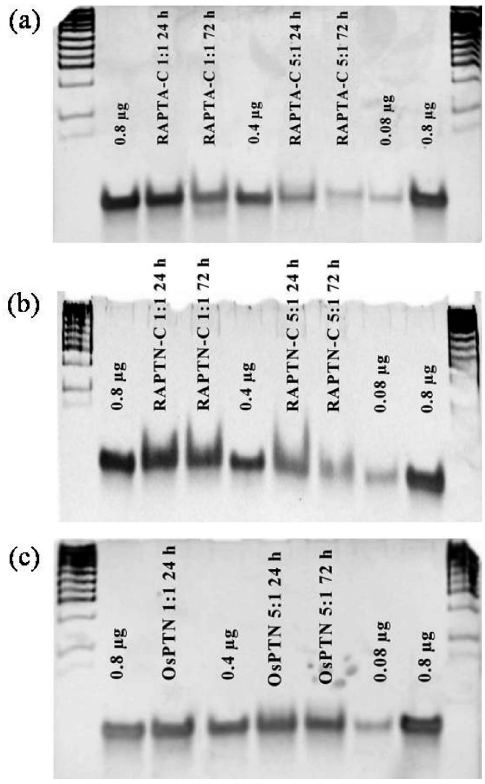

Figure 5. Gel electrophoresis of RAPTA-C (a), **1**·Cl (b), and **5**·Cl (c) following incubation for 24 and 72 h with oligonucleotide at ratios of 1:1 and 5:1. Equal amounts of the oligonucleotide (0.8 μg) were placed on the gel together with standards of 0.8, 0.4, and 0.08 μg. RAPTA-C degrades the oligonucleotide most effectively, **1**·Cl only at a drug to oligonucleotide ratio of 5:1, and **5**·Cl does not degrade the oligonucleotide.

Table 3. IC_{50} Values for 1·Cl−5·Cl and RAPTA-C in A2780 Cells

complex	IC_{50} (μM)
1·Cl	278 ± 12
2·Cl	179 ± 8
3·Cl	154 ± 11
4·Cl	203 ± 5
5·Cl	>500
ptn	>500
RAPTA-C	353 ± 12

order **3**·Cl > **2**·Cl > **4**·Cl > **1**·Cl ≫ **5**·Cl (Table 3). A similar trend is observed in RAPTA compounds, with the toluene derivative also showing the highest activity.[28] The osmium complex is significantly less cytotoxic than its ruthenium equivalent, possibly the result of slower ligand exchange kinetics, a feature also observed for other Ru/Os analogues.[53] The MS studies suggest that loss of the chloride ligand is the first step in binding to a potential biomolecular target, and accordingly the more active compounds, **2**·Cl and **3**·Cl, were those which showed the highest percentage of aqua species. It is noteworthy that **1**·Cl−**4**·Cl are all more cytotoxic than RAPTA-C, although RAPTA-C is considerably more reactive in oligonucleotide and nucleotide binding studies, while showing an affinity for ubiquitin similar to that of **1**·Cl. Combined, these data suggest that proteins may be more important as in vitro targets than DNA for these compounds.

Other ruthenium drug candidates, such as NAMI-A, exhibit similar cytotoxicities, and while they are much less active in vitro than, for example, cisplatin, they show excellent activities in vivo.[15,28,54] For example, the least cytotoxic ruthenium compound in vitro is RAPTA-C; nevertheless, in vivo it is active against solid lung metastasis[28] and Ehrlich ascites carcinoma[54] in the absence of observable side effects.

Conclusions

A series of water-soluble compounds of the general formula $[M(\eta^6\text{-arene})(ptn)Cl]^+$ (M = Ru, Os) have been synthesized and their crystal structures, reactivity with model (potential) biomolecular targets, and cytotoxicities determined. The complexes are relatively resistant to hydrolysis and are stable even at high chloride concentrations and at low pH, making the possibility of a ring-opening activation mechanism under physiological conditions unlikely. The Ru-ptn complexes show in vitro activities and reactivity toward ubiquitin comparable to those of their pta analogues, although their reactivity toward DNA is lower, possibly due to a much slower rate of hydrolysis. It has previously been proposed that proteins are a more important target for RAPTA-type complexes than DNA,[55] which is consistent with the results described herein.

Experimental Section

The ptn ligand was prepared by sodium-mediated reduction of $[Me\text{-}pta]^+$, as previously described, and sublimed under vacuum prior to use.[56] The ruthenium and osmium chloro-bridged dimers and RAPTA-C were synthesized according to literature procedures.[16,57,58] All solvents were degassed prior to use. ^{1}H, ^{13}C, ^{15}N, and ^{31}P NMR spectra were recorded on a Bruker Avance II 400 spectrometer at room temperature. Spectra were referenced to the ^{1}H signal of the NMR solvent or by inclusion of an external reference: H_3PO_4 for ^{31}P NMR. ESI-mass spectra of the compounds were obtained in water or acetonitrile on a ThermoFinnigan LCQ Deca XP Plus quadrupole ion-trap instrument operated in positive ion mode over a mass range of *m/z* 150−1000. The ionization energy was set at 5.0 V and the capillary temperature at 150 °C.

General Method for the Preparation of Complexes 1−5. $[M(\eta^6\text{-arene})Cl_2]_2$ (M = Ru, Os; 0.29 mM) and ptn (0.58 mM) were refluxed in chloroform for 5 h. The resulting solution was filtered and the solvent volume reduced to 25%. The product was triturated with pentane and the resulting powder filtered and washed with pentane and diethyl ether. $[M(\eta^6\text{-arene})(ptn)Cl]BF_4$ complexes **1**·BF_4−**5**·BF_4 were obtained by addition of 1 equivalent $NaBF_4$ to a CH_2Cl_2 solution of the chloride analogues. The formed NaCl was filtered off and the product was precipitated by addition of pentane, filtered and dried *in vacuo*.

[Ru(η^6-p-cymene)(ptn)Cl]Cl (1·Cl). Yield: 231 mg (85%), red powder. Slow diffusion of pentane into a CH_2Cl_2 solution of $[Ru(\eta^6\text{-}p\text{-cymene})(ptn)Cl]BF_4$ (**1**·BF_4) afforded crystals suitable for structural analysis by X-ray diffraction.

^{1}H NMR (400.13 MHz, D_2O, 25 °C; δ, ppm): 6.23 (m, 2H, Ar C*H*), 5.06 (m, 2H, Ar C*H*), 4.78 (d, 1H, $^2J_{HH}$ = 12.0 Hz, bridgehead N−C*H*H−N), 4.19−3.74 (m, 6H, CH_2), 3.49 (dd, 2H, $^2J_{PH}$ = 12.0 Hz, $^2J_{HH}$ = 8.0 Hz, N−C*H*H−P), 2.97 (d, 1H, $^2J_{HH}$ = 12.0 Hz, bridgehead N−CH*H*−N), 2.89 (s, 3H, N−CH_3), 2.70 (sept, 1H, $^3J_{HH}$ = 6.8 Hz, Ar C*H*$(CH_3)_2$), 2.14 (s, 3H, Ar CH_3), 1.83 (d, 3H, $^2J_{PH}$ = 12.0 Hz, P−CH_3), 1.21 (d, 3H, $^3J_{HH}$ = 6.8 Hz, Ar CH(CH_3)$_2$), 1.11 (d, 3H, $^3J_{HH}$ = 6.8 Hz, Ar CH(CH_3)$_2$). ^{31}P{^{1}H} NMR (D_2O, 161.98 MHz; δ, ppm): −27.9. ESI-MS (H_2O, positive ion mode; *m/z*): 443.9 $[Ru(\eta^6\text{-}p\text{-cymene})(ptn)Cl]^+$ (100%).

(54) Chatterjee, S.; Kundu, S.; Bhattacharyya, A.; Hartinger, C. G.; Dyson, P. J. *J. Biol. Inorg. Chem.* **2008**, *13*, 1149−1155.
(55) Dyson, P. J.; Sava, G. *Dalton Trans.* **2006**, 1929–1933.
(56) Assmann, B.; Angermaier, K.; Paul, M.; Riede, J.; Schmidbaur, H. *Chem. Ber.* **1995**, *128*, 891–900.
(57) Zelonka, R. A.; Baird, M. C. *Can. J. Chem.* **1972**, *50*, 3063–3072.
(58) Bennett, M. A.; Smith, A. K. *J. Chem. Soc., Dalton Trans.* **1974**, 233–241.

[Ru(η^6-C_6H_6)(ptn)Cl]Cl (2·Cl). Yield: 161 mg (70%), orange-brown powder. Slow diffusion of pentane into a CH_2Cl_2 solution of [Ru(η^6-C_6H_6)(ptn)Cl]BF_4 (**2**·BF_4) afforded crystals suitable for structural analysis by X-ray diffraction.

^{1}H NMR (400.13 MHz, CD_2Cl_2, 25 °C; δ, ppm): 5.94 (s, 6H, Ar C*H*), 4.79 (d, 1H, $^2J_{HH}$ = 12.0 Hz, bridgehead N−C*H*H−N), 4.25−3.75 (m, 6H, CH_2), 3.53 (dd, 2H, $^2J_{PH}$ = 14.0 Hz, $^2J_{HH}$ = 12.0 Hz, N−C*H*H−P), 3.40 (d, 1H, $^2J_{HH}$ = 12.0 Hz, bridgehead N−CH*H*−N), 2.99 (s, 3H, N−CH_3), 1.92 (d, 3H, $^2J_{PH}$ = 14.0 Hz, P−CH_3). ^{31}P{^{1}H} NMR (161.98 MHz, D_2O, 25 °C; δ, ppm): −28.7. ESI-MS (H_2O, positive ion mode; *m*/*z*): 352.9 [Ru(η^6-C_6H_6)(ptn)]$^+$ (10%), 369.9 [Ru(η^6-C_6H_6)(H_2O)(ptn) − H]$^+$ (10%), 387.9 [Ru(η^6-C_6H_6)(ptn)Cl]$^+$ (100%).

[Ru(η^6-$C_6H_5CH_3$)(ptn)Cl]Cl (3·Cl). Yield: 227 mg (87%), orange powder. Slow diffusion of diethyl ether into a methanol solution of [Ru(η^6-$C_6H_5CH_3$)(ptn)Cl]BF_4 (**3**·BF_4) afforded crystals suitable for structural analysis by X-ray diffraction.

^{1}H NMR (400.13 MHz, D_2O, 25 °C; δ, ppm): 6.27 (m, 2H, Ar *o*-C*H*), 6.04 (m, 1H, *p*-C*H*), 5.85 (m, 2H, *m*-C*H*), 4.87 (d, 1H, $^2J_{HH}$ = 5.6 Hz, bridgehead N−C*H*H−N), 4.25−3.78 (m, 6H, CH_2), 3.54 (dd, 2H, $^2J_{PH}$ = 14.0 Hz, $^2J_{HH}$ = 9.0 Hz, N−C*H*H−P), 3.15 (d, 1H, $^2J_{HH}$ = 5.6 Hz, bridgehead N−CH*H*−N), 2.91 (s, 3H, N−CH_3), 2.09 (s, 3H, Ar CH_3), 1.98 (d, 3H, $^2J_{PH}$ = 9.0 Hz, P−CH_3). ^{31}P{^{1}H} NMR (161.98 MHz, D_2O, 25 °C; δ, ppm): −28.0. ESI-MS (H_2O, positive ion mode; *m*/*z*): 367.1 [Ru(η^6-$C_6H_5CH_3$)(ptn)]$^+$ (5%), 383.8 [Ru(η^6-$C_6H_5CH_3$)(H_2O)(ptn) − H]$^+$ (15%), 401.9 [Ru(η^6-$C_6H_5CH_3$)(ptn)Cl]$^+$ (100%).

[Ru(η^6-C_6Me_6)(ptn)Cl]Cl (4·Cl). Yield: 215 mg (72%), red-brown powder. Crystals suitable for structural analysis by X-ray diffraction were obtained by slow diffusion of pentane into a CH_2Cl_2 solution of [Ru(η^6-C_6Me_6)(ptn)Cl]BF_4 (**4**·BF_4).

^{1}H NMR (400.13 MHz, D_2O, 25 °C; δ, ppm): 4.94 (m, 1H, bridgehead N−C*H*H−N), 4.45−3.53 (m, 8H, CH_2) 3.40 (m, 1H, bridgehead N−CH*H*−N), 2.99 (s, 3H, N−CH_3), 1.92 (d, 3H, $^2J_{PH}$ = 14.4 Hz, P−CH_3), 1.55 (s, 18H, Ar CH_3). ^{31}P{^{1}H} NMR (161.98 MHz, D_2O, 25 °C): δ −31.7 ppm. ESI-MS (MeCN, positive ion mode; *m*/*z*): 454.3 [Ru(η^6-$C_{12}H_{18}$)(H_2O)(ptn) − H]$^+$ (20%), 472.0 [Ru(η^6-$C_{12}H_{18}$)(ptn)Cl]$^+$ (100%).

[Os(η^6-C_6H_6)(ptn)Cl]Cl (5·Cl). Yield: 261 mg (86%), yellow powder. A microcrystalline powder of [Os(η^6-C_6H_6)Cl(ptn)]BF_4 (**5**·BF_4) was obtained by slow diffusion of ether into a methanol solution; however, the sample diffracted weakly.

^{1}H NMR (400.13 MHz, D_2O, 25 °C; δ, ppm): 6.02 (s, 6H, Ar C*H*), 5.08 (d, 1H, $^2J_{HH}$ = 12.4 Hz, bridgehead N−CH*H*−N), 4.42−3.87 (m, 6H, CH_2), 3.79 (dd, 2H, $^2J_{PH}$ = 14.8 Hz, $^2J_{HH}$ = 8.0 Hz, N−CH*H*−P), 3.14 (d, 1H, $^2J_{HH}$ = 12.4 Hz, bridgehead N−C*H*H−N), 3.08 (s, 3H, N−CH_3), 1.85 (d, 3H, $^2J_{PH}$ = 12.0 Hz, P−CH_3). ^{31}P{^{1}H} NMR (161.98 MHz, D_2O, 25 °C; δ, ppm): −77.8. ESI-MS (H_2O, positive ion mode; *m*/*z*): 460.0 [Os(η^6-C_6H_6)(H_2O)(ptn) − H]$^+$ (5%), 477.9 [Os(η-C_6H_6)(ptn)Cl]$^+$ (100%).

X-ray Structure Determination. Suitable single crystals were selected and manipulated in a perfluoro poly(alkyl ether) oil matrix (F06206K, ABCR Co.). The crystals were mounted on the end of a glass fiber attached to a metal pin fixed to a goniometer head which was placed in the Euler cradle, while a cold blanket of N_2 gas was maintained. The data for structures **1**·BF_4, **3**·BF_4, and **4**·BF_4 were collected on a Nonius KappaCDD diffractometer equipped with a Bruker-Apex II CCD area detector and an Enraf-Nonius FR590 X-ray generator and the data for **2**·BF_4 were collected on an Oxford-Kuma Kappa diffractometer with a Sapphire CCD area detector. All instruments utilize a graphite-monochromated Mo Kα radiation source with λ = 0.710 73 Å. The crystals were kept under a 140 or 100 K gaseous flow of N_2 during the collection procedure. For **1**·BF_4, **3**·BF_4, and **4**·BF_4, the unit cell and orientation matrix were determined by indexing reflections measured from phi/chi scans and analyzed with the program DIRAX,[59] while for **2**·BF_4 the unit cell was determined from the entire data set using CrysAlis RED.[60] All data sets are based on collecting reflections using an optimized scanning strategy utilizing the programs CollectCCD[61] and CrysAlis CCD (for **2**·BF_4 only). After data integration with either EvalCCD[62] or CrysAlis RED (**2**·BF_4), a multiscan absorption correction based on a semiempirical method was applied using the SADABS[63] or ABSPACK (a subprogram of CrysAlis RED) program. Space group determination was performed with the XPREP program.[64] A structure solution based on the direct-methods algorithm was employed with SHELXS-97.[65] Afterward, anisotropic refinement of all non-hydrogen atoms was completed on the basis of a least-squares full-matrix method against F^2 data using SHELXL-97.[66] Hydrogen atoms were added in geometrically calculated positions and refined as a riding model using a scaled thermal parameter to the connecting atom. In all cases, positional disordering of the terminal P and N atoms of the ptn was observed, which was resolved by splitting the atoms over two positions and allowing the total occupancy of the disordered groups to freely refine (details described in the CIF files in the Supporting Information). In some cases, the thermal parameters of some atoms were isotropically restrained. A small number of reflections in some cases were removed when $\Delta(F_o^2 - F_c^2)/\sigma$ exceeded 10.0. Important data for all structures are given in Table 4. Drawings were produced with ORTEP-3.[67]

Hydrolysis Studies. The hydrolytic stability of compounds **1**·Cl−**5**·Cl (1 mM) was determined in D_2O at 37 °C by ^{1}H and ^{31}P NMR spectroscopy. The pHs of the solutions were between 5.4 and 5.8.

Protein and (Oligo)nucleotide Binding Studies. (a) Sample Preparation. The HPLC-purified double-stranded 13-mer oligonucleotide ds(5′-GTATTGGCACGTA-3′) was bought as an aqueous solution with a concentration of 0.2 mM from A/S Technology (Denmark) and checked by polyacrylamide gel electrophoresis (PAGE) for complete annealing. RAPTA-C, **1**·Cl, and **5**·Cl were dissolved in water and immediately incubated with the oligonucleotide at effective complex to oligonucleotide ratios of 10:10 and 50:10 μM in a total volume of 300 μL in Eppendorf vials in a thermomixer (300 rpm; Eppendorf) at 37 °C. Evaporation was minimized by sealing the tubes with Parafilm and covering them with several layers of aluminum foil. Aliquots of 100 μL were taken after 1 and 3 days and stored at −20 °C until analysis by mass spectrometry or PAGE. The aqueous samples were thawed completely, and an aliquot of 5 μL was diluted 1:10 with a 1.1 mM solution of ammonium acetate in water−*n*-propanol−methanol (20:5:65), resulting in a final DNA concentration of 1 μM immediately prior to analysis. DNA was ionized with 1.8−2 kV in negative ion mode and 0.4 psi pressure. The XCalibur software (version 2.0.5) was used for data analysis and was also applied for offline recalibration of the full scan mass spectra, using the charge distributions (4- to 9-fold negatively charged) of single-stranded TACGTGCCAATAC.

For the protein-binding studies, **1**·Cl, **5**·Cl, and RAPTA-C were incubated with ubiquitin (from bovine red blood cells, minimum 90%; Sigma) at a molar ratio of 2:1, and samples were taken after 24 and 72 h incubation at 37 °C. The samples were diluted 1:100

(59) Duisenberg, A. J. M. *J. Appl. Crystallogr.* **1992**, *25*, 92–96.
(60) CrysAlis CCD and CrysAlis RED, Version 1.71; Oxford Diffraction Ltd, Abingdon, U.K., 2006.
(61) COLLECT: Data Collection Software; Bruker AXIS BV, Delft, The Netherlands, 1999.
(62) Duisenberg, A. J. M.; Kroon-Batenburg, L. M. J.; Schreurs, A. M. M. *J. Appl. Crystallogr.* **2003**, *36*, 220–229.
(63) Sheldrick, G. M. SADABS: Area Detector Absorption and Other Corrections, version 2.06; Bruker-AXS, Madison, WI, 2003.
(64) XPREP: Reciprocal Space Exploration, Version 6.14; Bruker-AXS, Madison, WI, 2003.
(65) Sheldrick, G. M. SHELXS-97, Program for Crystal Structure Solution; University of Göttingen, Göttingen, Germany, 1997.
(66) Sheldrick, G. M. SHELXL-97, Program for Crystal Structure Refinement; University of Göttingen, Göttingen, Germany, 1997.
(67) Farrugia, L. J. *J. Appl. Crystallogr.* **1997**, *30*, 565.

Table 4. Selected Crystallographic Data for $1\cdot BF_4$−$4\cdot BF_4$

	$1\cdot BF_4$	$2\cdot BF_4$	$3\cdot BF_4$	$4\cdot BF_4$
formula	$C_{17}H_{30}RuPN_3ClBF_4\cdot CH_2Cl_2)$	$C_{13}H_{22}RuPN_3ClBF_4$	$C_{14}H_{23}RuPN_3ClBF_4$	$C_{19}H_{34}RuPN_3ClBF_4$
fw	687.73	474.64	488.66	558.79
color, habit	orange, prismatic	orange, irregular	orange, prismatic	orange, prismatic
cryst syst	orthorhombic	triclinic	monoclinic	orthorhombic
space group	$Pna2_1$	$P\bar{1}$	$P2_1/c$	$Pnma$
a, Å	12.6112(13)	12.4204(12)	8.7241(9)	9.5739(16)
b, Å	12.8196(15)	12.8918(14)	15.7830(16)	12.9609(9)
c, Å	15.4543(11)	13.3447(18)	13.8016(13)	18.1197(13)
α, deg	90	113.158(11)	90	90
β, deg	90	108.410(10)	103.171(9)	90
γ, deg	90	101.856(9)	90	90
V, Å^3	2498.5(4)	1730.0(3)	1850.4(3)	2248.4(4)
Z	4	4	4	4
cryst dimens, mm^3	0.430 × 0.174 × 0.113	0.27 × 0.25 × 0.24	0.417 × 0.261 × 0.189	0.297 × 0.197 × 0.072
d_{calcd}, g cm^{-3}	1.828	1.828	1.754	1.651
μ, mm^{-1}	1.065	1.198	1.119	0.932
no. of rflns	51 795	10 310	36 207	38 876
R(int)	0.0687	0.0347	0.0736	0.0962
no. of obsd rflns	4391	5205	3254	2104
min/max transmissn	0.6950	0.778 20	0.5698	0.6950
R1 ($I > 2\sigma(I)$)	0.0277	0.0381	0.0511	0.0366
R1 (all data)	0.0352	0.0592	0.0624	0.0673
wR2 ($I > 2\sigma(I)$)	0.0481	0.0839	0.1054	0.0497
wR2 (all data)	0.0510	0.0938	0.1099	0.0729
no. of restraints	1	6	0	0
no. of params	293	451	230	165
goodness of fit on F^2	1.094	1.018	1.222	1.140
resid electron density, e Å^{-3}	0.474, −0.391	0.658, −0.744	0.790, −0.744	0.502, −0.500

with H_2O−CH_3CN−HCOOH (70:30:1) and immediately analyzed by mass spectrometry. The mass spectra were recalibrated using the different charge states of ubiquitin in the positive ion mode as internal standards.

(b) Mass Spectrometry. For electrospray ionization mass spectrometry, the samples were placed into a 96-well plate in an Advion TriVersa robot (Advion Biosciences, Ithaca, NY) equipped with a 5.5 μm nozzle chip. The ESI robot was controlled with ChipSoft v7.2.0 software employing the following parameters: gas pressure 0.40 psi; voltage 1.8−2.0 kV; sample volume 10 μL. The samples were analyzed in negative ion mode using a hyphenated ion-trap-FT-ICR mass spectrometer comprising an LTQ XL and an 11 T FT-ICR MS (both ThermoFisher Scientific, Bremen, Germany). The Xcalibur software bundle was utilized for data acquisition (Tune Plus version 2.2 SP1; ThermoFisher Scientific) and data analysis (Qual Browser version 2.2; ThermoFisher Scientific). Mass spectra were recorded at a resolution of 75 000 at m/z 500 for m/z 350−2000. A single scan consisted of 5 microscans, and the spectrum was averaged over at least 50 scans. In addition to full scan ion trap and FT-ICR mass spectra, protein binding data were collected in WSIM mode (m/z 770−870).

(c) Gel Electrophoresis. Samples were thawed, and 10 μL aliquots (0.8 μg of oligonucleotide) were mixed with 2 μL of 6X sample buffer and completely loaded on a native 20% polyacrylamide gel. Puc-mix (smallest oligonucleotide 45 bp) was used as mass ruler in the two outermost lanes, and pure double-stranded DNA of sequence ds(GTATTGGCACGTA) was used in amounts of 0.8, 0.4, and 0.08 μg as standards for estimation of the concentration of the oligonucleotide upon incubation. 1X TBE buffer was used as electrolyte, and electrophoresis was performed at a constant current (12 mA) for 3−4 h. Gels were stained with ethidium bromide (0.5 μg/mL) for 15−20 min and visualized under UV.

Cell Line and Culture Conditions. The human A2780 ovarian cancer cell line was obtained from the European Collection of Cell Cultures (Salisbury, U.K.). Cells were grown routinely in RPMI medium containing glucose, 5% fetal calf serum (FCS), and antibiotics at 37 °C and 5% CO_2.

Determination of Cell Viability (MTT Assay). Cytotoxicity was determined using the MTT assay (MTT = 3-(4,5-dimethyl-2-thiazolyl)-2,5-diphenyl-2*H*-tetrazolium bromide). Cells were seeded in 96-well plates as monolayers with 100 μL of cell solution (approximately 20 000 cells) per well and preincubated for 24 h in medium supplemented with 10% FCS. Compounds were dissolved directly in the culture medium to the appropriate concentration, with the exception of $4\cdot$Cl, which was added as a DMSO solution and serially diluted to the appropriate concentration (to give a final DMSO concentration of 0.5%). A 100 μL portion of the drug solution was added to each well, and the plates were incubated for another 72 h. Subsequently, MTT solution (0.2 mg/mL) was added to the cells and the plates were incubated for a further 2 h. The culture medium was aspirated, and the purple formazan crystals formed by the mitochondrial dehydrogenase activity of vital cells were dissolved in DMSO. The optical density, directly proportional to the number of surviving cells, was quantified at 540 nm using a multiwell plate reader, and the fraction of surviving cells was calculated from the absorbance of untreated control cells. Evaluation is based on means from two independent experiments, each comprising three microcultures per concentration level.

Acknowledgment. We are indebted to the EPFL, the Swiss National Science Foundation, the University of Vienna, the FWF−Austrian Science Fund (CGH Schrödinger Fellowship J2613-N19), and COST D39 for financial support. This research was supported by Marie Curie Intra European Fellowships within the 6th and 7th European Community Framework Programme projects MEIF-CT-2005-025287-CARCAS (A.D.P.) and 220890-SuRuCo (A.A.N.). We thank Dr. Rosario Scopelliti for collecting the X-ray data and Prof. Yury O. Tsybin for use of the FT-ICR-MS.

Supporting Information Available: CIF files giving crystallographic data for $1\cdot BF_4$−$4\cdot BF_4$. This material is available free of charge via the Internet at http://pubs.acs.org.

OM800899E